Composite Structures 88 (2009) 394–402

Contents lists available at ScienceDirect

Composite Structures

journal homepage: www.elsevier.com/locate/compstruct

An electromechanical Reissner–Mindlin model for laminated piezoelectric plates

Lin Liao, Wenbin Yu *

Mechanical and Aerospace Engineering Department, Utah State University, Logan, 84322-4130, USA

ARTICLE INFO

Article history:
Available online 1 May 2008

Keywords:
Variational asymptotic method
Piezoelectric plate
Reissner–Mindlin

ABSTRACT

An electromechanical Reissner–Mindlin model is constructed for laminated piezoelectric plates using the variational asymptotic method. This model is applicable to laminates without prescribed electric potential through the thickness. Taking advantage of the smallness of the plate thickness, we rigorously split the original 3D piezoelectricity problem into a 1D through-the-thickness analysis and a 2D plate analysis, and both are fully-coupled electromechanical analyses. Examples of single layer and multi-layer plates have been used to demonstrate the accuracy and application of this model.

1. Introduction

Considerable amount of research and investigation have been done to study laminated piezoelectric plates. The exact solutions of laminated piezoelectric plates can be obtained analytically for a few cases of ideal material type, geometry, and boundary conditions [1–3]. For general cases, we can use the three-dimensional (3D) multiphysics finite element method (FEM) to find numerical solutions [4]. However, it is labor intensive to prepare the 3D multiphysics FEM model for a laminated piezoelectric plate, especially if it is composed of many anisotropic layers with different orientations. Moreover, the prohibitive computational cost of 3D FEM can only be justified for detailed analyses and prevents its use in design and overall simulation of realistic engineering systems involving such components. Numerous two-dimensional (2D) plate models have been constructed in order to simplify the analysis of piezoelectric plates, which generally start from some assumptions for the through-the-thickness distribution of the 3D field quantities. According to the way the assumptions applied, piezoelectric plate models can be classified as equivalent single-layer models [5–17] if the assumptions are applied to the entire structure and layerwise models [18–21] if the assumptions are applied to each layer. In the past investigation, single-layer theory of mechanical fields is usually combined with layerwise approximation of electric potential [22–25], and 2D finite element is incorporated in developing these plate theories [22,23,26]. In addition, considerable efforts have been dedicated to the study of vibration suppression, shape control, and buckling enhancement, and optimization of composite plates with embedded or surface bonded piezoelectric actuators/sensors [27–29]. These models have two main disadvantages: (1) the *a priori* assumptions which are natural extensions from isotropic, homogeneous structures cannot be easily justified for highly heterogeneous and anisotropic structures such as laminated piezoelectric plates; (2) there is no rational way for the analyst to determine the loss of accuracy and which refinement (i.e. single-layer versus layerwise, first-order versus higher-order) should be used for a reasonable tradeoff between accuracy and efficiency.

Extensive researches have been done on piezoelectric plates with electroded face surfaces and interfaces between layers [30] so that the electric potential can be prescribed at a certain point through the thickness. However, it is also possible that no electric potential is prescribed at any point through the thickness, say the electrodes are coated on the lateral boundary of the plate. The research works on this electrode arrangement are associated with transducers and resonators, which oftentimes belong to the area of electrical engineering or physics. It is noted that the lateral field excitation can also be produced by placing two electrodes on the same face surface of the plate [31–34], which might be one of the reasons that study on the case of electroded lateral boundary has not received much attention. Most of the investigations for this type of loading have been devoted to the study on vibration modes, depolarizing-field effect, electromechanical coupling coefficients, and admittance [35–38]. Published works related to the mechanics of piezoelectric composite plates with electroded lateral edges are rare. In particular, static analysis of displacements, strains, and stresses has not been found in the literature. Even for prescribed electric load on the lateral boundary, the electric field is often specified as a constant instead of a field generated by prescribed electric potential along the electroded edges [39].

The focus of this paper is to construct a generalized Reissner–Mindlin model with both electric and mechanical measures for laminated piezoelectric plates without prescribed electric potential through the thickness. The variational asymptotic method (VAM)

* Corresponding author. Tel.: +1 435 7978246; fax: +1 435 7972417.
E-mail address: wenbin.yu@usu.edu (W. Yu).

0263-8223/$ - see front matter © 2008 Elsevier Ltd. All rights reserved.
doi:10.1016/j.compstruct.2008.04.017

[40] will be applied to mathematically split the coupled 3D electromechanical analysis into a series of one-dimensional (1D) electromechanical through-the-thickness analyses and 2D electromechanical analyses over the reference plane. The coupled through-the-thickness analyses calculate both the mechanical warping and the electric warping, the meaning of which will be defined later. The results of the coupled through-the-thickness analyses are generalized 2D electric enthalpy, which can be transformed into the form of a generalized Reissner–Mindlin model. The coupled through-the-thickness analyses can also provide a set of recovery relations to reproduce 3D distribution of the electromechanical fields within the structure based on the results obtained from the 2D electromechanical analysis. One of the major applications of 2D plate models developed is the computation of resonant frequencies of piezoelectric devices [41].

2. Three-dimensional formulation

The Hamilton's extended principle for a piezoelectric composite plate can be written as

$$\int_{t_1}^{t_2} [\delta(\mathscr{K} - \mathscr{H}) + \overline{\delta \mathscr{W}}] \mathrm{d}t = 0 \tag{1}$$

where t_1 and t_2 are arbitrary fixed times, $\mathscr{K}$ and $\mathscr{H}$ are the kinetic energy and electric enthalpy, respectively, $\overline{\delta \mathscr{W}}$ is the virtual work of applied loads and electric charges (if exist). The bar is used to indicate that the virtual work need not be the variations of functionals.

For piezoelectrics, the electric enthalpy can be expressed as

$$\mathscr{H} = \frac{1}{2} \int_{\mathscr{V}} (\boldsymbol{\Gamma}^T : \boldsymbol{C}^{\boldsymbol{E}} : \boldsymbol{\Gamma} - 2\boldsymbol{E} \cdot \boldsymbol{e} : \boldsymbol{\Gamma} - \boldsymbol{E}^T \cdot \varepsilon^{\Gamma} \cdot \boldsymbol{E}) \mathrm{d}\mathscr{V} \tag{2}$$

where $\boldsymbol{C}^E$ is the elastic tensor at constant electric field, $\boldsymbol{\Gamma}$ is the strain tensor, $\boldsymbol{e}$ is the piezoelectric tensor, $\boldsymbol{E}$ is the electric field vector, ε^{Γ} is the dielectric tensor at constant strain field, and $\mathscr{V}$ is the space occupied by the structure. Although we are focusing on plates made of piezoelectrics, the present formulation is equally applicable to smart structures made of other active materials characterized by a constitutive model with the same mathematical structure.

As sketched in Fig. 1, a point in the plate can be described by its Cartesian coordinates x_i, where x_α are two orthogonal lines in the reference plane and x_3 is the normal coordinate. (Here and throughout the paper, Greek indices assume values 1 and 2 while Latin indices assume 1, 2, and 3. Repeated indices are summed over their range except where explicitly indicated.) Letting $\mathbf{b}_i$ denote the unit vector along x_i for the undeformed plate, one can then describe the position of any material point in the undeformed configuration by its position vector $\hat{\mathbf{r}}$ from a fixed point O, such that

$$\hat{\mathbf{r}}(x_1, x_2, x_3) = \mathbf{r}(x_1, x_2) + x_3 \mathbf{b}_3 \tag{3}$$

where $\mathbf{r}$ is the position vector from O to the point located by x_α on the reference plane. When the reference plane of the undeformed plate coincides with its middle plane, we have

$$\langle \hat{\mathbf{r}}(x_1, x_2, x_3) \rangle = h \mathbf{r}(x_1, x_2) \tag{4}$$

where the angle-brackets denote the definite integral through the thickness of the plate, denoted as h. The position vector of any material point in the deformed plate $\hat{\mathbf{R}}$ can be represented as

$$\hat{\mathbf{R}}(x_1, x_2, x_3) = \mathbf{R}(x_1, x_2) + x_3 \mathbf{B}_3(x_1, x_2) + w_i(x_1, x_2, x_3) \mathbf{B}_i(x_1, x_2) \tag{5}$$

where $\mathbf{R}$ is the position vector of the reference plane for the deformed plate, $\mathbf{B}_i$ is an orthonormal triad for the deformed configuration, and w_i are warping functions introduced to accommodate all possible deformation other than those described by $\mathbf{R}$ and $\mathbf{B}_i$. To ensure a unique expression for $\hat{\mathbf{R}}$ in terms of $\mathbf{R}$, $\mathbf{B}_i$, and w_i, we need to introduce six constraints. We can define $\mathbf{R}$ to be the average position through the plate thickness, which implies that the warping functions must satisfy the following three constraints

$$\langle w_i(x_1, x_2, x_3) \rangle = 0 \tag{6}$$

Another two constraints can be specified by choosing $\mathbf{B}_3$ as the normal to the reference plane of the deformed plate. It should be noted that this choice has nothing to do with the famous Kirchhoff hypothesis, in which no local deformation of the transverse normal is allowed. Here, we have accommodated all possible deformation using the warping functions.

Because $\mathbf{B}_\alpha$ can freely rotate around $\mathbf{B}_3$, we can introduce the last constraint as

$$\mathbf{B}_1 \cdot \mathbf{R}_{,2} = \mathbf{B}_2 \cdot \mathbf{R}_{,1} \tag{7}$$

Based on the concept of decomposition of rotation tensor [42], we can obtain 3D strains valid for small local rotations using

$$\Gamma_{ij} = \frac{1}{2}(F_{ij} + F_{ji}) - \delta_{ij} \tag{8}$$

where δ_{ij} is the Kronecker symbol, and F_{ij} is the mixed-basis component of the deformation gradient tensor such that

$$F_{ij} = \mathbf{B}_i \cdot \mathbf{G}_k \mathbf{g}^k \cdot \mathbf{b}_j \tag{9}$$

with $\mathbf{G}_k$ as the covariant base vectors of the deformed configuration and $\mathbf{g}^k$ as the contravariant base vectors of the undeformed configuration. The 2D generalized strains $\varepsilon_{\alpha\beta}$ and $K_{\alpha\beta}$ can be defined as

$$\begin{aligned} \mathbf{R}_{,\alpha} &= \mathbf{B}_\alpha + \varepsilon_{\alpha\beta} \mathbf{B}_\beta \\ \mathbf{B}_{i,\alpha} &= (-K_{\alpha\beta} \mathbf{B}_\beta \times \mathbf{B}_3 + K_{\alpha 3} \mathbf{B}_3) \times \mathbf{B}_i \end{aligned} \tag{10}$$

Using Eq. (8) along with Eqs. (9), (10), (5) and (3), we can express the 3D strain field Γ_{ij} in terms of $\varepsilon_{\alpha\beta}$, $K_{\alpha\beta}$, and w_i. For geometrically nonlinear analysis, we can assume that the strains are small compared to unity and warpings are of the order of strain or smaller. Neglecting higher-order terms, one can express the 3D strain field as

$$\begin{aligned} \Gamma_e &= \varepsilon + x_3 \kappa + I_1 w_{\|,1} + I_2 w_{\|,2} \\ 2\Gamma_s &= w'_{\|} + e_1 w_{3,1} + e_2 w_{3,2} \\ \Gamma_t &= w'_3 \end{aligned} \tag{11}$$

where $()' = \frac{\partial ()}{\partial x_3}$, $()_{\|} = \lfloor ()_1 ()_2 \rfloor^{\mathrm{T}}$

$$\Gamma_e = \lfloor \Gamma_{11}\ 2\Gamma_{12}\ \Gamma_{22} \rfloor^{\mathrm{T}} \quad 2\Gamma_s = \lfloor 2\Gamma_{13}\ 2\Gamma_{23} \rfloor^{\mathrm{T}} \quad \Gamma_t = \Gamma_{33}$$

$$\varepsilon = \lfloor \varepsilon_{11}\ 2\varepsilon_{12}\ \varepsilon_{22} \rfloor^{\mathrm{T}} \quad \kappa = \lfloor K_{11}\ K_{12} + K_{21}\ K_{22} \rfloor^{\mathrm{T}}$$

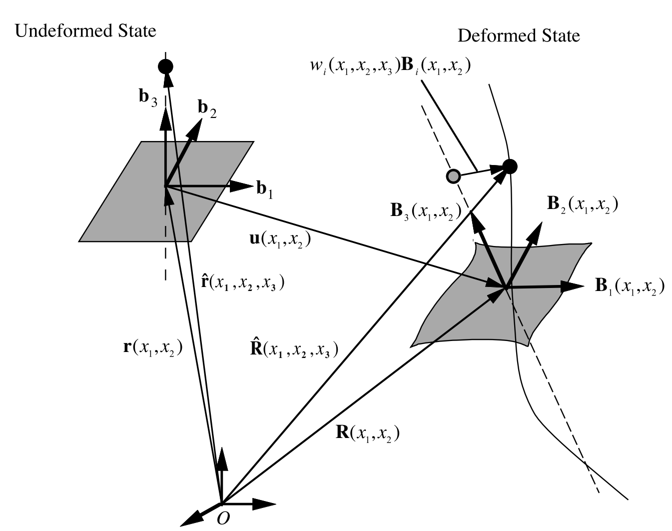

Fig. 1. Schematic of plate deformation.